

ANALYSIS OF FIBER ORIENTATION, MICROSTRUCTURE AND MECHANICAL PROPERTIES OF SPECIMENS MADE FROM FIBER-REINFORCED ABS MANUFACTURED BY FUSED FILAMENT FABRICATION (FFF)

Kay A. Weidenmann¹, Sascha Baumann², Pascal Pinter¹ and Peter Elsner^{1,2}

¹Institute for Applied Materials, Karlsruhe Institute of Technology, Kaiserstr. 12, 76137 Karlsruhe, Germany

Email: kay.weidenmann@kit.edu, Web Page: <http://www.iam.kit.edu/wk>

Email: pascal.pinter@kit.edu, Web Page: <http://www.iam.kit.edu/wk>

²Fraunhofer Institute for Chemical Technology, Joseph-von-Fraunhofer-Str. 7, 76327 Pfinztal, Germany

Email: sascha.baumann@ict.fraunhofer.de, Web Page: <http://www.ict.fraunhofer.de>

Email: peter.elsner@ict.fraunhofer.de, Web Page: <http://www.ict.fraunhofer.de>

Keywords: Fused Filament Fabrication, Fibre Reinforced Polymers, Fiber Orientation, Mechanical Properties, X-ray computed tomography

Abstract

Fused filament fabrication (FFF) is a state-of-the-art process for manufacturing polymer-based components by 3D-printing. Unfortunately, conventional acrylonitrile-butadiene-styrene (ABS) materials used in FFF processes feature relatively low strength and hardness in comparison to materials used in injection molding. This contribution aims on the systematic, quantitative analysis of the fiber orientation in specimens manufactured from fiber-reinforced ABS by fused filament fabrication and its impact on the mechanical properties. ABS based compounds featuring different fiber contents have been compounded and subsequently processed by FFF. The microstructure of the composite materials have been analyzed regarding the fiber orientation using X-ray computed tomography. It could be stated, that the short fibers are oriented according to the printing paths and hence serve as markers for the analysis of the printing path course. To evaluate the mechanical properties, samples with different printing path course and therefore different fiber orientations have been manufactured. Bending tests and impact bending tests were carried out to compare the mechanical properties of reinforced samples in comparison to ABS materials without fibers. In general, an impact of fiber volume content and fiber orientation could be found for the specimens investigated.

1. Introduction

Additive Manufacturing of structural parts allows for more freedom in component construction and enhances the potential for lightweight design. ABS represents a state-of-the art material for fused filament fabrication (FFF) representing a popular process in polymer additive manufacturing. It is well known, that incorporating fibers in polymers may enhance the mechanical properties. Nevertheless, FFF is based on the continuous lay-up of single strands resulting in joint lines in the manufactured parts mar the mechanical properties. Therefore, reincreasing the mechanical properties by incorporating fibers represents a promising strategy to overcome this problem. Only a few research

studies report on fiber-reinforced polymers processed in FFF have been published. Zhong et.al. [1] have shown that incorporating short glass fibers in polymer blends based on ABS and polyethylene results in an increase in mechanical properties. Fibre contents investigated were in the range of 10 to 18 wt.%. However, not pure ABS but a polymer blend was used in this case. With printing paths oriented perpendicular to the testing direction in tensile tests, a decrease of tensile strength was observed. The improvement (of up to 100%) was observed in tensile tests with printing paths being parallel oriented to the tensile direction. A further increase in strength could be found for carbon fiber reinforced ABS [2-4]. Shofner et.al. [2] compounded 10 wt% of carbon nanofibers in ABS resulting in an increase of roundabout 40% in tensile strength. However, such nanofibers could be rather considered to be a filler than a fiber reinforcement. Ning et.al. [3] used short carbon fibers in reinforced ABS-based filaments and investigated the impact of fibre content, fibre length and porosity on the mechanical properties investigated in bending and tensile tests. They found an increase in mechanical properties at low fiber contents (up to 7.5 wt%) followed by a decrease of the tensile strength up to a fibre content of 15 wt.% representing the limit of their study. Indeed, it was shown, that an increase in fiber content is accompanied by a decrease of the ductility of the specimens in tensile tests. This was led back to an steady increase of the porosity in the sample, which was calculated from the specimen volume and its fiber content. Tekinalp et.al. [4] used short (0.2 – 0.4 mm) carbon fibers in reinforced ABS-based filaments and investigated both the fibre orientation in the printed specimens and its impact on the mechanical properties. They found a fiber orientation above 90% in the direction of printing. However, fiber orientation was derived from a 2D orientation analysis based on plastography featuring a relatively low accuracy in comparison to 3D methods like X-ray computed tomography. Indeed, the published studies state, that the FFF process has an impact on the fibre orientation in printed specimens resulting in an impact on the mechanical properties. The aim of this contribution is to use 3D-microcomputed tomography for the analysis of fiber orientation in specimens fabricated by FFF. For this purpose, a good contrast in X-ray adsorption is helpful to separate the fibers from the surrounding matrix. Therefore, the study presented here is based on glass fiber reinforced ABS. The microstructure of the composite materials have been analyzed regarding the fiber orientation based on Pinter et.al. [5] using X-ray computed tomography. To evaluate the mechanical properties, samples with different printing path course and therefore different fiber orientations and different fiber contents (0 wt.%, 5 wt.% and 10 wt.%) have been manufactured. Bending tests and impact bending tests were carried out to compare the mechanical properties of short glass fibre reinforced samples in comparison to specimens made from neat ABS.

2. Experimental

2.1. Filament Fabrication

The filament used in this study was fabricated by extrusion on a Leistritz ZSE 27 micro co-rotating twin screw extruder (cf. Figure 1) with a length-to-diameter ratio of 36. The materials used were neat ABS (Styrolution Terluan GP22) and ABS with 20 wt.% glass fiber content (Styrolution Terluan GP22G4).

Fiber contents were adjusted by premix procedure and filaments with 0 wt.%, 5 wt.% and 10 wt.% glass fiber were produced. The diameter of the fabricated filaments was 2.85 mm with a deviation of +/- 0.1 mm for neat ABS. Filaments with fibre contents were produced with a diameter of 2.5 mm with a deviation of +/- 0.2 mm.

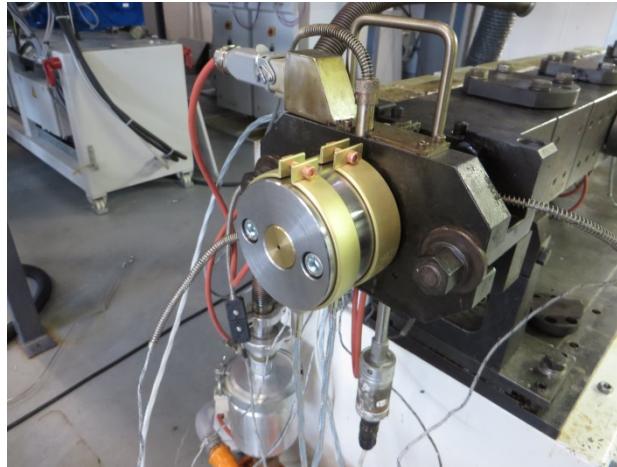


Figure 1. Leistritz ZSE 27 micro extruder with filament extrusion die

2.2. Specimen fabrication and geometry

Specimens were fabricated using a commercial FFF printer Ultimaker 2 using the standard printing parameters (buildplate temperature: 90 °C, nozzle temperature 250 °C) for ABS. The printer was modified regarding the nozzle diameter which was changed to 0.55 mm for this study. Preliminary tests with standard nozzle diameters of 0.2 mm have shown, that the short fibers amass inside the nozzle and interrupt the material flow.

For the bending test specimens lateral dimensions of 80x10 mm² were chosen at a sample thickness of 3 mm. For the impact bending tests, the specimens were rectangular featuring dimensions of 50x6x4 mm³. For the impact bending tests, specimens were printed both with the 50x6 surface (“flat”) or the 50x4 surface (“upright”) lying on the buildplate resulting in different printing path courses and hence fiber orientations inside the specimens. For all specimens manufactured, shell thickness and top/bottom thickness was chosen to be 1 mm resulting in UD-printing paths within these regions of the specimens. Hence, all samples are printed with printing paths being parallel to the circumference (with a thickness of 1 mm) and the inner structure printed in a diamond pattern at a fill density of 100 %.

2.2. Mechanical testing and CT analysis

The CT analysis was carried out on an YXLON precision computed tomography system containing an open X-ray reflection tube with tungsten target and a 2048 x 2048 pixel flat panel detector with a pixel pitch of 200 μm from Perkin Elmer. For the images acquired in this work, the tube parameters were set to a acceleration voltage of 80 kV and a target current of 0.01 mA. The resolution is 5.75 μm/voxel and thus, every single fiber in the image can be recognized separately.

This data was evaluated with the commercial software VGStudio Max 2.2, which offers the ability to calculate fiber orientation distributions (FODs) of fiber reinforced polymers. Therefore, the coordinate system was aligned in that way, that the z-axis matches the longitudinal axis of the specimen while the x-axis corresponds to the longer side of the base area.

Three point bending tests were carried out on a Zwick universal testing machine with a maximum load capacity of 2.5 kN according DIN EN ISO 178 using a lower support span of 48 mm and a support radius of 5 mm (cf. Figure 2). Crosshead velocity was chosen to be 1 mm/min, the flexural strength σ_c^f was determined at a flexural strain of 3.5%, tests would be stopped at a maximum flexural strain of 4.7% if the sample did not break at earlier strains. Bending modulus was determined in the range of 0.05% and 0.25% flexural strain using a linear approximation. The specimen surface which was touching the buildplate during the printing process was always oriented to the two lower supports. Six samples have been tested for each fibre content (0 wt.%, 5 wt.%, 10 wt.%)



Figure 2. Experimental setup of the 3-point-bending test.

The impact bending tests have been carried out on a Zwick Charpy tester with a maximum pendulum energy of 5 J. The support span was chosen to be 40 mm. The samples were always oriented flatwise with the pendulum hitting the 50x4 surface of the samples hence leading to different print path course orientations with respect to the test direction. The impact bending strength was calculated from the measured energy and the according sample dimensions.

3. Results

3.1. Bending tests

Representative stress-strain-diagrams for the different specimen configurations tested are shown in Figure 3. It is clearly visible, that an increase of the fibre content leads to a decrease of the maximum bending stress and of the maximum bending strain. For the ABS samples without fibre reinforcement, none of the bending samples fractured within the maximum bending strain applied of 4.7%. For samples with a glass fibre content of 5 wt.% 3 of 6 samples fractured at a strain limit close to 4.7%. All samples with a fibre content fractured at a maximum strain well below 4.5%. Hence, the increasing fibre content enhances embrittlement of the specimen. Additionally, flexural modulus decreases with increasing fibre volume content. Indeed, for all characteristics, the impact of the fibre volume content between 0 and 5 wt.% is less in comparison to a further increase from 5 to 10 wt.%.

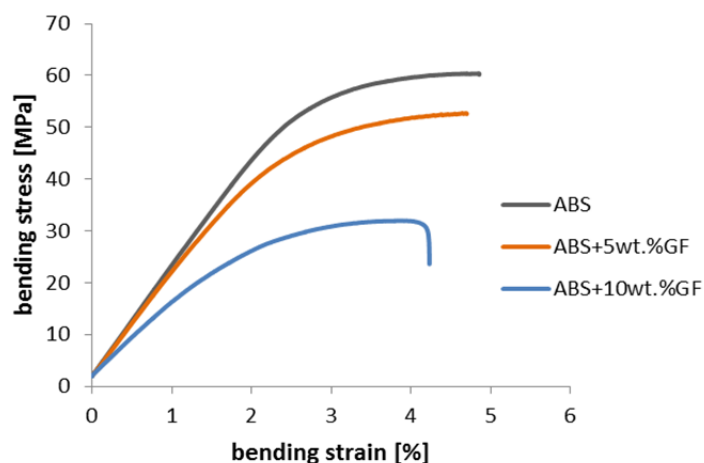


Figure 3. Representative stress-strain diagram for 3-pt-bending test on specimens featuring different fibre volume contents.

Table 1 sums up the results of the 3-point-bending tests.

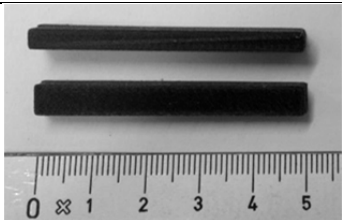
Table 1. Results of the 3-pt-bending tests.

Specimen Type	E (MPa)	σ_c (MPa)	No. of fractured samples (-)	fracture strain (%)
ABS	2036±70	56.4±2.7	0 of 6	-
ABS+5wt.%GF	2024±64	50.2±1.6	3 of 6	4.67±0.01
ABS+10wt.%GF	1546±119	33.2±3.0	6 of 6	4.02±0.23

3.2. Impact bending tests

The results of the impact bending tests are summarized in Table 2. For each fiber content both “flat” and “upright” (c.f. Chapter 2.2) have been tested.

Table 2. Results of the impact bending tests.

Specimen Type	Impact bending strength (kJ/m ²)	Sample orientations ("upright", above; "flat", below)
ABS, flat	33.0±7.8	
ABS, upright	40.2±9.1	
ABS+5wt.%GF, flat	10.3±1.2	
ABS+5wt.%GF, upright	9.1±0.9	
ABS+10wt.%GF, flat	5.4±1.4	
ABS+10wt.%GF, upright	5.8±1.1	

For non-reinforced samples, the impact bending strength tends to depend from the printing path course with “upright” samples being more ductile in comparison to “flat” samples. For the reinforced samples, there is no clear trend. In general, an increase of the fiber content reduces the impact bending strength.

3.3. Microstructure and fibre orientation analysis using CT

Figure 4 illustrates a slice of the upright printed specimen in the xz-plane with zero, five and ten weight percent glass fibers. The material was printed from the left to the right, so the left edge was connected to the heated groundplate of the printer. It can be seen that the porosity of the glass fiber filled material increases with the distance to the heated plate. The bulk material shows almost no porosity in the entire specimen. The resulting fiber orientation histograms are depicted as polar plots in Figure 5. It can be stated, that most of the fibers of all specimen are oriented to the z-direction. Flat printed specimen show two strong peaks in the x-plane with an angle of ±45° to the z-axis, what results from the 45° diamond pattern printing path from manufacturing. The upright printed specimen show almost similar peaks in the y-plane, but with lower intensity.

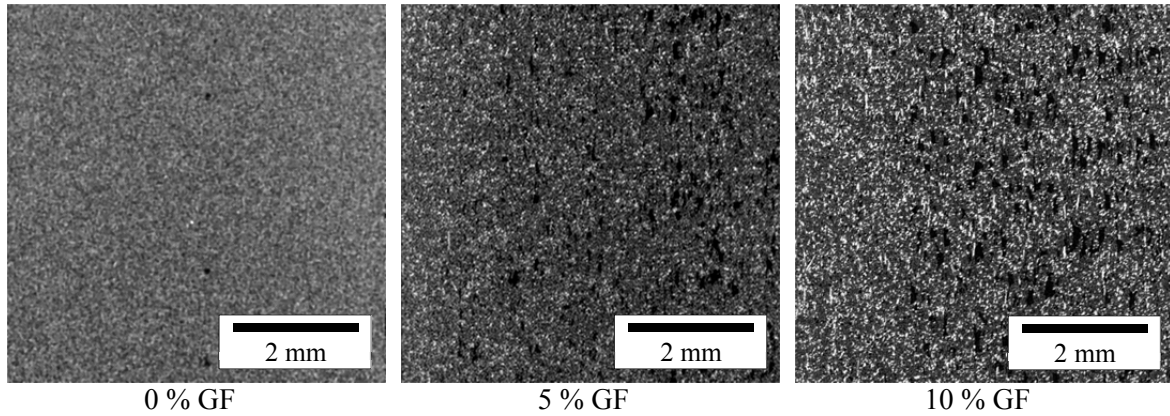


Figure 4. Microstructure analysis of printed specimen showing pores (black) and short fibres (white).

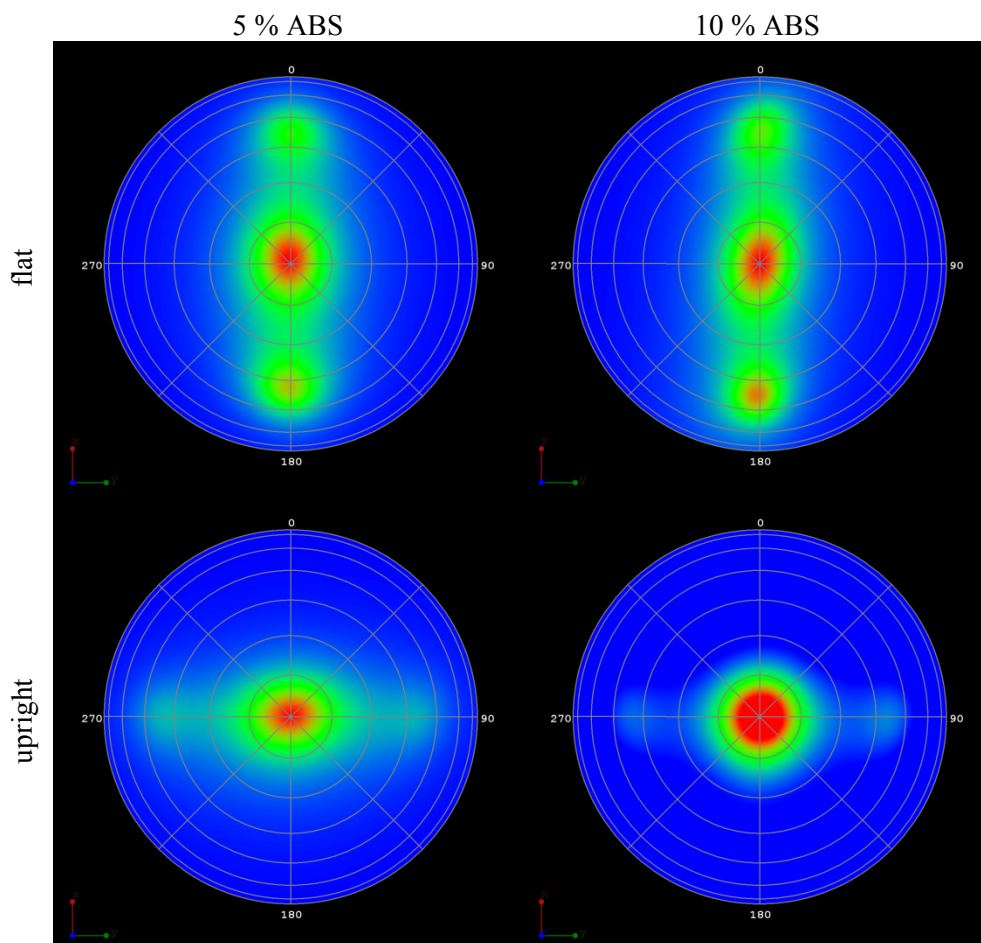


Figure 5. Fiber orientation distributions of investigated specimen.

4. Discussion

All samples are printed with printing paths being parallel to the circumference (with a thickness of 1 mm) and the inner structure printed in a diamond pattern. Therefore, for upright samples, the fraction of strands lying parallel to the direction of crack propagation is higher. In non-reinforced ABS the crack propagation is more effectively hindered in upright samples resulting in a higher impact bending strength as measured in the tests shown above. The bending tests showed, that both ductility and

strength in reinforced samples is reduced in comparison to non-reinforced ABS. The CT analysis (c.f. Figure 4) reveals that this may be due to porosity being present in reinforced samples. Consequently, the impact bending strength is reduced and the impact of printing path orientation on the impact bending strength is secondary in comparison with the porosity. Furthermore, the porosity of the fiber reinforced specimen depends of the distance to the heated ground plate. It is very likely, that this could be avoided by a different heating concept, i.e. a more homogeneous heating of the sample during the printing process.

Additionally, the CT analysis shows, that the short fibres are mostly oriented following the printing paths. Hence, the specimens contain fibres with UD orientation and fibres with $\pm 45^\circ$ orientation (c.f. Figure 5). Thereby, the “flat” samples feature a higher volume content of areas with diamond pattern resulting in more intensive $\pm 45^\circ$ peaks in the polar plots. This is due to the printing strategy: “Flat” samples are printed with the $50 \times 6 \text{ mm}^2$ surface lying on the buildplate. As the shell thickness is fixed to 1 mm (with the shell featuring UD printing paths), the ratio of diamond pattern to UD printing paths in the shell is roundabout 2:1 for “flat” samples. The ratio for “upright” samples is roundabout 1:1. Hence, the polar plots of “upright” samples show weaker peaks at orientations of $\pm 45^\circ$ peaks. For this reason, the impact bending strength is expected to be higher for a larger volume fraction oriented in z-direction, where the principal stress occurs (c.f. Figure 6). However, for a reasonable approach, the moment of inertia has to be calculated with respect to the local fiber volume fraction and orientation. Although the flat printed samples show a lower volume fraction aligned to the z-axis, the oriented areas are located on the edges with maximum distance to the neutral fiber, what could finally lead to a higher moment of inertia and consequently to better global mechanical properties if the formation of pores during printing could be avoided.

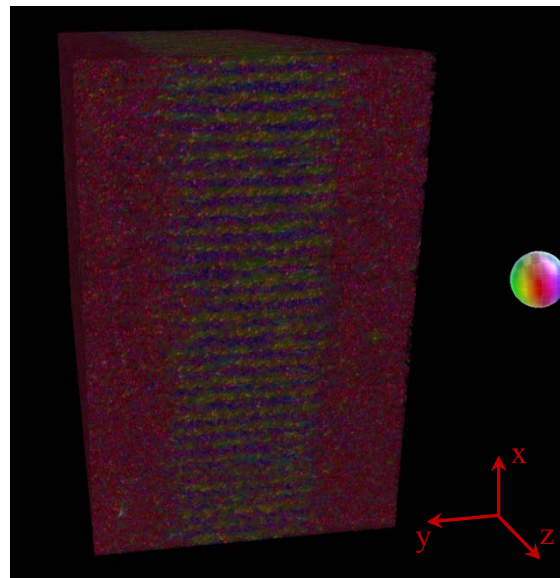


Figure 6. Fiber orientation distribution in an “upright” printed specimen reveals the layered structure with UD orientation in the outer shells (purple) and the diamond pattern layers in $\pm 45^\circ$ -layers (yellow/blue). The visible xy-plane has the dimensions of a crosssection through the entire specimen (4 x 6 mm).

In general, the decrease of the mechanical properties in comparison and in contrary to preliminary reports [1-4], may be due to differences in printing procedures (heating concept) and material optimization. Zhong et.al. [1] used a polymer blend, which could have been optimized to avoid porosity in the printed components. The impact of porosity on mechanical properties has already been found by [3] and is in good coincidence with the results presented here.

5. Conclusions

From the results presented and discussed, the following conclusions can be drawn:

- In short fibre reinforced samples fabricated by FFF, the incorporated short fibres are oriented following the printing paths.
- The glass short fibres feature a good adsorption contrast and hence serve as indicators for the printing path analysis using CT analysis.
- Fibre reinforced filaments may be used in FFF but optimization of the printing process (heating) and the material composition are necessary to get pore free components.
- Porosity, printing path and hence fibre orientation influence the resulting mechanical properties of samples fabricated by FFF.
- The problem of pore formation is correlated to an increasing fibre content.

Further investigations on this research topic should focus on modified batch compositions to avoid porosity formation. Nevertheless, high fibre contents reduce the printability of polymers in FFF significantly.

Acknowledgments

The authors acknowledge the partial support by the German Research Foundation (DFG) within the International Research Training Group “Integrated engineering of continuous-discontinuous long fiber reinforced polymer structures“ (GRK 2078).

References

- [1] W. Zhong, F. Li, Z. Zhang, L. Song, Z. Li. Short fiber reinforced composites for fused deposition modeling, *Materials Science and Engineering: A*, 301:125-130, 2001
- [2] M.L. Shofner, K. Lozano, F.J. Rodriguez-Macias, E.V. Barrera. Nanofiber-reinforced polymers prepared by fused deposition modeling, *Journal of Applied Polymer Science*, 89:3081–3090, 2003
- [3] F. Ning, W. Cong, J. Qiu, J. Wei, S. Wang. Additive manufacturing of carbon fiber reinforced thermoplastic composites using fused deposition modeling, *Composites Part B: Engineering* 80: 369–378, 2015
- [4] H.L. Tekinalp, V. Kunc, G.M. Velez-Garcia, C.E. Duty, L.J. Love, A.K. Naskar, C.A. Blue, S. Ozcan. Highly oriented carbon fiber–polymer composites via additive Manufacturing, *Composite Science and Technology* 105:144-150, 2014
- [5] P. Pinter, S. Dietrich, K.A. Weidenmann. Algorithms for the Determination of Orientation-Tensors from Three Dimensional μ CT Images with Various Microstructures, *Proceedings of the 20th International Conference on Composite Materials ICCM-20, Copenhagen, Denmark, July 19-24 2015* (<http://iccm20.org/fullpapers/file?f=REnD1W4BYW>)